Journal of Zhejiang University SCIENCE A
ISSN 1673-565X (Print); ISSN 1862-1775 (Online)
www.zju.edu.cn/jzus; www.springerlink.com
E-mail: jzus@zju.edu.cn

Fibrous TiO_2 prepared by chemical vapor deposition using activated carbon fibers as template via adsorption, hydrolysis and calcinations*

Hui-na YANG[1], Li-fen LIU[†‡2], Feng-lin YANG[2], Jimmy C. YU[3]

([1]*School of Chemical Engineering, Dalian University of Technology, Dalian 116023, China*)

([2]*School of Environmental and Biological Science and Technology, Dalian University of Technology, Dalian 116023, China*)

([3]*Department of Chemistry, the Chinese University of Hong Kong, Hong Kong, China*)

[†]E-mail: yuzhe25521@yahoo.com.cn

Received Nov. 26, 2007; revision accepted Apr. 8, 2008

Abstract: TiO_2 fibers were prepared via alternatively introducing water vapor and Ti precursor carried by N_2 to an APCVD (chemical vapor deposition under atmospheric pressure) reactor at ≤200 °C. Activated carbon fibers (ACFs) were used as templates for deposition and later removed by calcinations. The obtained catalysts were characterized by scanning electron microscopy (SEM), transmission electron microscopy (TEM), Brunauer, Emmett and Teller (BET) and X-ray diffraction (XRD) analysis. The pores within TiO_2 fibers included micro-range and meso-range, e.g., 7 nm, and the specific surface areas for TiO_2 fibers were 141 m^2/g and 148 m^2/g for samples deposited at 100 °C and 200 °C (using ACF1700 as template), respectively. The deposition temperature significantly influenced TiO_2 morphology. The special advantages of this technique for preparing porous nano-material include no consumption of organic solvent in the process and easy control of deposition conditions and speeds.

Key words: Chemical vapor deposition (CVD), Porous material, Activated carbon fiber (ACF)
doi:10.1631/jzus.A0720089 **Document code:** A **CLC number:** TQ134.1; TQ085

INTRODUCTION

In recent years, porous metal oxides have attracted a great deal of attention in many fields, such as heterogeneous catalysis (Savage, 2000; Anandana *et al.*, 2006), sensors (Caricato *et al.*, 2007), solar cells (Kondo *et al.*, 2008) and supports (Macak, 2007). TiO_2 is the most widely used and studied photocatalyst due to its chemical stability and availability. Its preparation methods include sol-gel, flame pyrolysis, hydrothermal, as well as chemical vapor deposition (CVD), precipitation, etc. (Imai *et al.*, 2004; Madhugiri *et al.*, 2004; Yuan *et al.*, 2006a; Liu *et al.*, 2007). Using the conventional sol-gel method to prepare highly porous TiO_2 requires a high consumption of organic solvents, and the electrolytic method for TiO_2 nanotube uses expensive titanium plate. Thus, preparing highly active nano-material by a clean, low cost and low consumption process is desirable.

High surface area hollow TiO_2 fibers are easy to recover and separate, with low tendency of agglomeration. Techniques such as electric-spinning (Viswanathamuithi *et al*., 2004; Madhugiri *et al.*, 2004), ion-exchange approach (Liu *et al*., 2007), and template approach (Imai *et al.*, 2002; Lu *et al.*, 2005; Yuan *et al.*, 2006b) for TiO_2 fibers have been studied. The template approaches are simple and versatile in fiber size control, such as heating the impregnated activated carbon fiber (ACF) templates (Yuan *et al.*, 2006b) and supercritical treatment (Yuan *et al*., 2006) with either solvent or high pressure.

In this study, hollow TiO_2 fibers with high specific surface area and sometimes floatable were prepared through low temperature chemical vapor deposition under atmospheric pressure (APCVD)

‡ Corresponding author
* Project (No. 20477006) supported by the National Natural Science Foundation of China

using ACF as templates, without consuming any organic solvent, which, to our knowledge, has not been reported before. The entire preparation is inexpensive and easy to perform. Titanium tetrachloride ($TiCl_4$), a liquid with a high vapor pressure (1.87 kPa at 298 K), much cheaper than organic precursors such as titanium tetraisopropoxide (TTIP), is used as the precursor. In order to reduce the hydrolysis rate, $TiCl_4$ and water vapors were carried to the CVD reactor alternately by nitrogen (N_2). After deposition, hollow TiO_2 fibers were obtained by burning off ACF, which maintained the features of ACF structure and morphology. Effects of deposition temperature on TiO_2 configurations and shapes were investigated in this study.

EXPERIMENTAL

Materials

The ACF samples used in the experiment were made from polyacrylonitrile fiber, in felt form, with a Brunauer, Emmett and Teller (BET) specific surface area of 1100 m^2/g and 1700 m^2/g, respectively (abbreviated as ACF1100 and ACF1700), and micro-spore size of less than 1 nm and meso-pore around 2 nm. The fibers were cleaned by anhydrous alcohol to remove the adsorbed impurities and then washed by deionized water. After that, the fibers were dried at 105 °C in air for 6 h and activated at 200 °C in a tubular furnace under atmospheric pressure for 2 h.

All reagents (analytical grade) were purchased from Tianjin Reagent Corporation (Tianjin, China).

Synthesis process

The apparatus used for preparing TiO_2 fiber catalyst consists of an electric tubular furnace with a vertical quartz reactor tube inside. A schematic diagram of the reactor is shown in Fig.1.

The hollow TiO_2 fibers were prepared as follows. 1 g of activated ACF was put into the center of the quartz tube. N_2 was bubbled into containers half-filled with $TiCl_4$ solution and/or $NH_3{\cdot}H_2O$ (5%, w/w) solution, respectively, then carried $TiCl_4$ or NH_3 and water vapor into the reactor alternately. It is very important to introduce water vapor together with NH_3 to the reactor separately from the introduction of $TiCl_4$, to allow diffusion and adsorption by the template. Adsorbed water and NH_3 molecule reacted with the introduced $TiCl_4$. After completion of hydrolysis reaction, because of the depletion of absorbed water and NH_3, further introduced $TiCl_4$ molecules got adsorbed onto unoccupied ACF and the newly formed $Ti(OH)_4$ surface. At next round of introduction of water vapor, $TiCl_4$ molecules were hydrolyzed. This repeated cycle of adsorption, hydrolysis and deposit reactions, together with the release of formed HCl, possibly NH_4Cl as well, was maintained at different deposition temperature ((20±5) °C, 100 °C and 200 °C), by the temperature control monitor. The whole system was operated under atmospheric pressure. After deposition, calcinations of the composite fibers were carried out at 600 °C (ramp=5 °C/min) for 2 h. The resulting TiO_2 sample was denoted as TiO_2-*T*-1100, where *T* and 1100 represent the deposition temperature (°C) and ACF specific surface area (m^2/g), respectively. The total deposition time was 2 h. The interval between alternating introduction of water vapor and $TiCl_4$ was 5 min. Flow rate of N_2 for carrying $TiCl_4$ and $NH_3{\cdot}H_2O$ to the reactor was maintained at 100 or 150 ml/min.

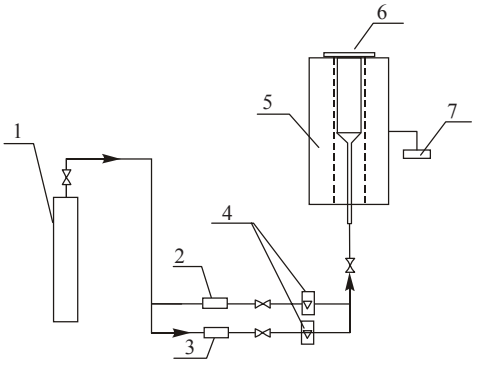

1: Nitrogen bottle; 2: Water evaporation chamber; 3: Precursor evaporation chamber; 4: Rotameter; 5: Tubular furnace; 6: Quartz tube; 7: Temperature control monitor

Fig.1 Schematic diagram of the CVD system

Characterization

Scanning electron microscopy (SEM) (JSM-5600LV instrument operated at 20 kV or 15 kV), transmission electron microscopy (TEM) (JSM-100CX II instrument operated at 200 kV), and X-ray diffraction (XRD, D/MAX-2400 X-ray diffractometer using Cu Kα irradiation, with a scan rate of 2° 2θ/min in the range of 5°~80°) were used for characterization of the prepared TiO_2 fibers. Their BET

specific surface area was determined via N_2 adsorption at 77 K on an Autosorb-1-MP. Before the measurement, all the samples were degassed at 350 °C for 4 h. The pore size distributions for micro- and meso-pores were calculated by Horvath-Kawazoe (HK) and Barret, Joyner and Halender (BJH) methods, respectively.

Photocatalytic activity

The photocatalytic activity was determined through the degradation of phenol in a 200 ml cylindrical shallow vessel with a quartz cover, irradiated by a 20 W low-pressure mercury lamp with major emission at 254 nm, located above the vessel. The photo catalytic test was carried out without any stirring or air bubbling, as the TiO_2 suspended well in the solution. The concentration of TiO_2 fibers was 0.1 g/L. The initial concentration of phenol was 50 mg/L. Prior to the irradiation, adsorption equilibrium of phenol on catalyst was reached after 0.5 h of catalyst addition. Then the light was turned on, and it was treated as the starting point (t=0) of the reaction and the corresponding phenol concentration was recorded as C_0. The concentration of phenol (C) was measured with the standard 4-aminoantipyrine calorimetric method.

RESULTS AND DISCUSSIONS

From SEM analysis of the formed TiO_2 at different deposit temperatures, using either ACF1100 or ACF1700 as template, the morphology difference of formed TiO_2 was observed. It was indicated that controlling deposition temperature and using a highly porous template were critical to the preparation of fibrous TiO_2.

Characterization of the prepared catalysts

The SEM micrographs of original ACF1100 and TiO_2-T-1100 are shown in Fig.2. Compared with original ACF (Figs.2a and 2b), the TiO_2 deposited at 20 °C (Figs.2c and 2d) was of flat sheet and acicular form, with some white floccules on TiO_2 surface, obviously because the deposition temperature was too low. However, fibrous TiO_2 was obtained by deposition at 20 °C using ACF1700 as template (figure not shown), as the porosity of ACF1700 was higher than that of ACF1100. This showed the importance and effect of template on formed TiO_2 and its structure. Hollow TiO_2 fibers were obtained at both 100 °C and 200 °C using ACF1100 or ACF1700 as template (figure not shown). From Figs.2e and 2f, it could be seen that TiO_2-200-1100 was hollow with a uniform outer diameter of about 7 μm and a length averaged at about 50 μm. The formed TiO_2 fiber maintained the feature of the templates, though with a diameter reduction and size shrinkage. The surface of catalyst deposition at 200 °C was rough and displayed several linear grooves and ridges aligned in the longitudinal direction, which replicated the original fibers faithfully. There were crinkle-like structures on the surface of TiO_2 fibers.

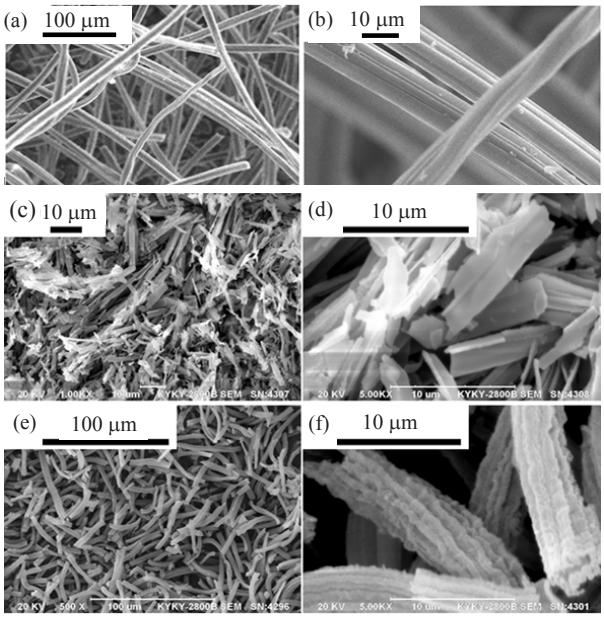

Fig.2 SEM images of (a), (b) original ACF1100; (c), (d) TiO_2-20-1100; and (e), (f) hollow structure of TiO_2-200-1100 with higher magnification

The morphology differences of catalysts deposited at different temperatures might be explained from two aspects. On one hand, the diffusion rates of precursor and water molecules were improved with the increase of temperature. The size of $TiCl_4$ molecule is about 0.132 nm, small enough to be adsorbed into the micro-pores of ACF (Matsumoto *et al.*, 1992). Relative easiness of diffusion into pores followed the order: macro-pores>meso-pores>micro-pores. The $TiCl_4$ molecule diffused onto ACF surface firstly and then diffused into pores of ACF, and hydrolyzed with

adsorbed water on ACF. The deposition reaction at 20 °C took place largely on outer surface of ACF1100 because the diffusion rate of $TiCl_4$ and water vapor into the pores might be limited. Thus, a small and flat sheet TiO_2 was obtained. At higher deposition temperature, such as 200 °C, vapor molecules reached the inner and deeper pores of ACF through diffusion, the template was used more efficiently, and more porous hollow TiO_2 fibers were obtained finally. On the other hand, at a high deposition temperature, release of hydrogen chloride, water vapor and/or ammonium chloride formed during hydrolysis reaction was improved, too, together with the increase of diffusion rate of precursors. However, except those deposited TiO_2 and $Ti(OH)_4$ on the surface of ACF, most hydrolysis by-products such as NH_4Cl, could not be released timely at a low deposition temperature, and the pores of ACF might get plugged, which affected the diffusion to the inner pores of ACF.

The morphology differences of TiO_2-20-1100 and TiO_2-20-1700, or TiO_2-200-1100 arose from the different pore sizes between ACF1100 and ACF1700 samples. Hydrolysis of $TiCl_4$ was easy and fast when water vapor was present even at room temperature, so the TiO_2 morphology was largely controlled by diffusion of precursors, which was affected by the ACF pore structure. As the larger BET specific surface area of ACF template is, the more porous the ACF fibers get, this high porosity allows penetration of precursors and water vapor. The ACF model structure and fractal pore images (Huang *et al.*, 2002; Zeng *et al.*, 2005) help better understand the structure and morphology of formed TiO_2 fibers. The catalyst is deposited via precursor and vapor diffusion into the pores of ACF then hydrolytic reaction, and it finally takes shape via thoroughly releasing the by-products and removing template ACF during calcinations. Thus, the channel between the pores within ACF in a way shapes the morphology of the formed TiO_2.

The TEM analysis of TiO_2 fibers was shown in Fig.3. The observed fibers appearance is shown in Fig.3a. The cross sectional image of the fiber edge is shown in Figs.3b and 3c. The particle size of TiO_2 fibers was uniform, at about 20 nm, and inside there were still tiny arrays of crystals and voids (as the arrows point out), which is very special to TiO_2 structures. A clear image of crystal structure (Fig.3b) and a column shaped porous structure (~5 nm) (Fig.3c) are shown. Large irregular pores with a width of 10~20 nm between the crystals were also found in the TEM (Figs.3b and 3c), which was in agreement with the pore size distribution (Fig.5). It also showed that trace residual carbon was still present. The structure and functional groups on the surface of ACF pores were not even in molecular level, such as the micro-graphite area and the area rich in oxygen-containing functional groups. The functional groups included basic types and acidic types, which might promote or inhibit hydrolysis/deposition in the initial stage of deposition differently. Thus an uneven, rough look of catalyst and small crystal structure in the particle was obtained. Another possible explanation for this phenomenon was that the ammonium chloride formed during deposition might not decompose until 324 °C to leave space behind. This led to formation of a larger number of small sized crystals during the subsequent calcinations process.

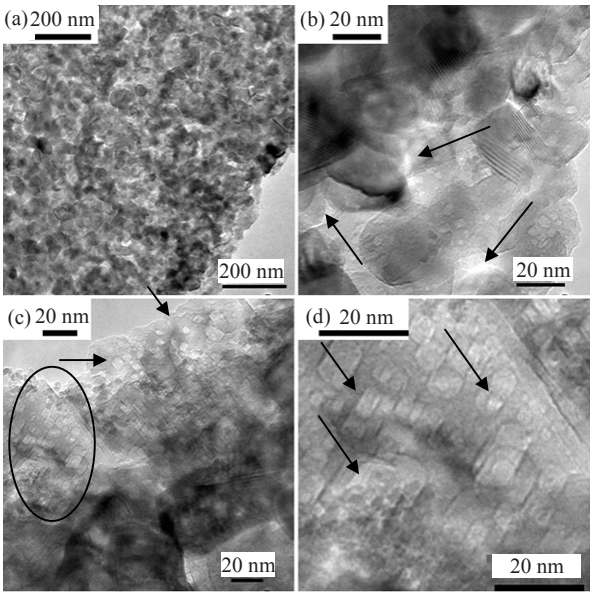

Fig.3 TEM images of TiO_2-100-1100. (a) Appearance; (b) Cross section; (c) Edge and (d) Left side of (c)

The wide-angle XRD pattern of the TiO_2 fiber (Fig.4) indicated that the catalyst crystal was in the anatase phase, and the higher deposition temperature favored the formation of smaller size particles, as there were broadened main peaks. TiO_2-200 had wider peaks at around 38° than TiO_2-100 or TiO_2-20 (Fig.4b, ACF1100). Also a smaller crystal size of TiO_2-200 than that of TiO_2-20 was obtained using ACF1700 as template (Fig.4a). There might be trace

signal from graphite structure in residual carbon, since its peak (2θ=23°) was weak and very close to the anatase peak at 2θ=25.3°.

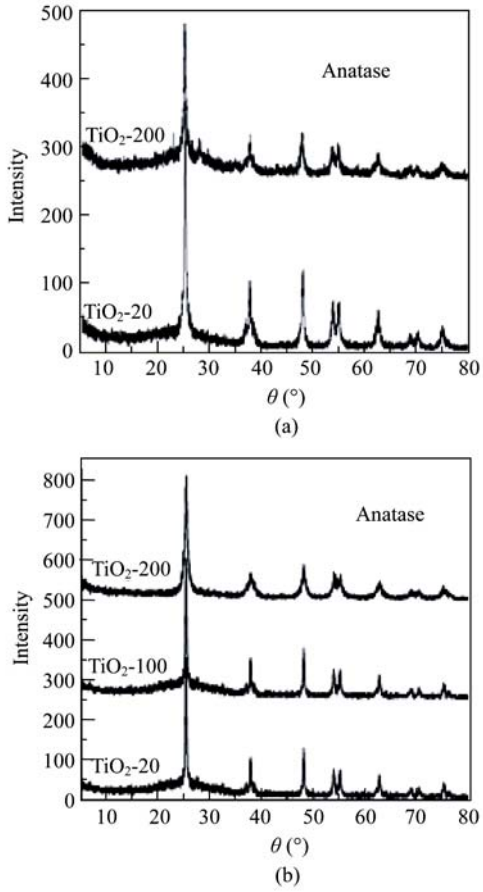

Fig.4 XRD patterns of (a) TiO_2-*T*-1700 and (b) TiO_2-*T*-1100

The nitrogen adsorption isotherms, micro- and meso-pore size distribution curves for TiO_2-100-1700 and TiO_2-200-1700 are shown in Fig.5. The BET specific surface areas of TiO_2-100-1700 and TiO_2-200-1700 were 141.0 m^2/g and 148.2 m^2/g, respectively. It is indicated that the precursors permeated into pores of the ACF and deposited on the carbon wall in the initial stage of deposition, and that the TiO_2 layer grew thicker as the deposition continued. Followed calcinations reactions removed most of the carbons, leaving irregular pores shaped by the carbon wall.

From pore size distribution analysis, it could be seen that the two samples were similar in micro- and meso-pores distributions, peaked at 0.5 nm (Fig.5b) and 7 nm (Fig.5c), respectively. At a closer look at the pore distribution, it is found that the pore volume was higher for TiO_2-200 than for TiO_2-100 in both the micro-pore and meso-pore ranges, and that a sharper peak of pore volume around 7 nm was observed in TiO_2-200-1700 (Fig.5b).

BET analysis of other TiO_2 samples showed that the higher the porosity of ACF was, the higher the BET specific surface area of TiO_2 fibers deposited at the same temperature, the deposition temperature (20, 100 or 200 °C) and the BET specific surface of the formed TiO_2 were using the same ACF template.

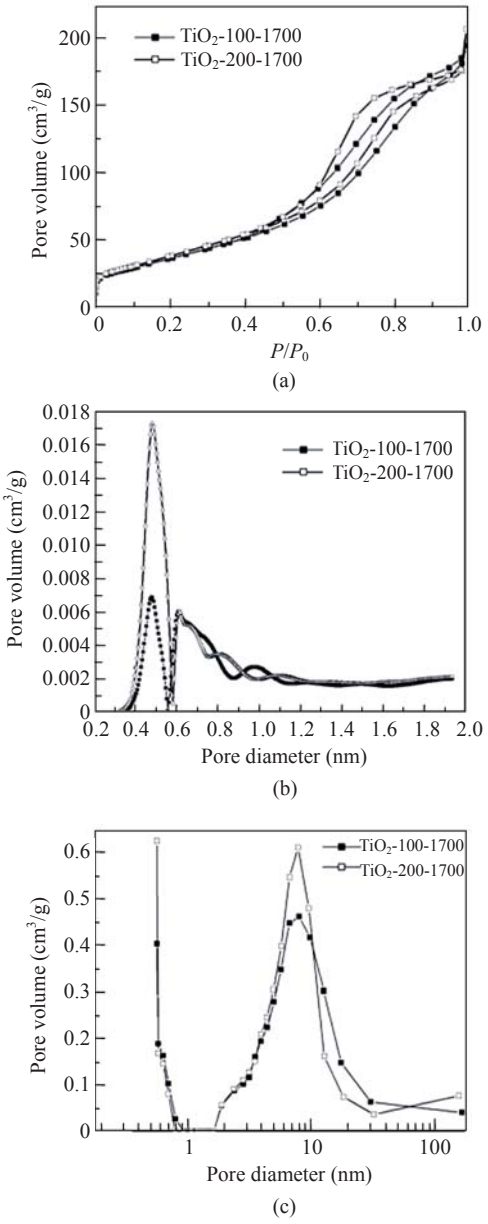

Fig.5 N_2 adsorption/desorption isotherms (a), micro-pore (b) and meso-pore (c) size distributions for TiO_2-100-1700 and TiO_2-200-1700

An interesting phenomenon was observed: some fibrous TiO_2 readily floated (TiO_2-100-1700 and TiO_2-100-1700) and suspended well in water without precipitation, while others could not float such as TiO_2-20-1100 (deposited at 20 °C, using ACF1100). This possibly depended on the proportions of sealed pores. More careful characterization needs to be done to draw a firm conclusion.

Photocatalytic activity

The adsorption of phenol (initial, for all tests at 50 mg/L) onto TiO_2 fibers took place as they were mixed, so 30 min adsorption after mixing was allowed to reach a relatively stable equilibrium. Then the concentration of remaining phenol solution before the start of UV (ultraviolet) irradiation was determined (C_0). The total removed phenol concentration by adsorption ($50-C_0$) and photocatalysis (C_0-C) was determined and compared by measuring the phenol concentration (C) changes. C/C_0 as y-axis decreased versus adsorption time and photocatalysis time, as shown in Fig.6. For different TiO_2 fibers, C_0 was different.

The TiO_2-200-1700 exhibited higher removal of phenol than TiO_2-100-1700 and TiO_2-20-1700 (Fig.6). It might be because TiO_2-200-1700 had larger surface area and smaller particle size compared with the other two samples. In addition, the larger amount of meso-pores favored diffusion of the phenol inside TiO_2. The TiO_2-200-1700 had higher adsorption capacity for phenol, thus a lower equilibrium concentration than that of TiO_2-20-1700 was observed (Fig.6). Although the difference of C/C_0 is not very great, actually the concentration difference is quite big if expressed in mg/L. If C/C_0 differs by 0.1~0.2, it means a concentration difference of 5~10 mg/L. The accuracy of measurement may reach 0.01 mg/L.

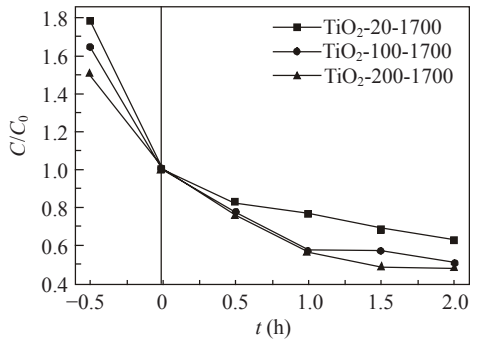

Fig.6 Photocatalytic phenol removal from water using TiO_2 deposited at different temperatures using ACF1700 as template

For designing an economic catalyst preparation process, the carrier gas could be reused first by passing through water to remove any un-reacted precursors and by-products, followed by a drying process to remove moistures.

Synthesized TiO_2 fibers may find promising applications as gas sensors, self-cleaning/regenerating adsorbent, and catalyst support. In addition to their excellent structure properties, porous materials may offer a high adsorption and retention potential towards aqueous pollutants or gaseous substances. This developed process can also be easily adapted to the syntheses of other oxides with interesting catalytic or sensing properties, such as SnO_2, ZrO_2, CeO_2, etc.

CONCLUSION

Hollow TiO_2 fiber was prepared with an APCVD method using ACF as template. TiO_2 was first deposited into the pore of ACF, followed by repeated introduction of water vapor and Ti precursor alternatively at a relatively low temperature, then the ACF was burnt off by calcinations. Both the pore structure of ACF and the deposition temperature had important influences on morphology and structure of TiO_2. The ACF characteristics shaped the TiO_2 deposition by its pore size and surface functional groups, while the deposition temperature determined deposition dynamics. Irregular hollow TiO_2 fibers were a typical product deposited at 200 °C. The secondary particle size was about 20 nm, with pores distributed in micro-, meso- and macro-ranges, which endowed the catalyst with better adsorption and photocatalytic activity in removing phenol pollutant from water. The preparation of fibers of nano-materials in this work was simple and easy.

References

Anandan, S., Vinub, A., Venkatachalam, N., Arabindoo, B., Murugesan, V., 2006. Photocatalytic activity of ZnO impregnated Hβ and mechanical mix of ZnO/Hβ in the degradation of monocrotophos in aqueous solution. *Journal of Molecular Catalysis A Chemical*, **256**(1-2): 312-320. [doi:10.1016/j.molcata.2006.05.012]

Caricato, A.P., Capone, S., Ciccarella, G., Martino, M., Rella,

R., Romano, F., Spadavecchia, J., Taurino, A., Tunno, T., Valerini, D., 2007. TiO_2 nanoparticle thin film deposition by matrix assisted pulsed laser evaporation for sensing applications. *Applied Surface Science*, **253**(19):7937-7944. [doi:10.1016/j.apsusc.2007.02.066]

Huang, Z., Kang, F., Huang, W., Yang, J., Liang, K., Cui, M., Cheng, Z., 2002. Pore structure and fractal characteristics of activated carbon fibers characterized by using HRTEM. *Journal of Colloid and Interface Science*, **249**(2):453-457. [doi:10.1006/jcis.2002.8274]

Imai, H., Matsuta, M., Shimizu, K., Hirashima, H., Negishi, N., 2002. Morphology transcription with TiO_2 using chemical solution growth and its application for photocatalysts. *Solid State Ionics*, **151**(1-4):183-187. [doi:10.1016/S0167-2738(02)00708-7]

Kondo, Y., Yoshikawa, H., Awaga, K., Murayama, M., Mori, T., Sunada, K., Bandow, S., Iijima, S., 2008. Preparation, photocatalytic activities, and dye-sensitized solar-cell performance of submicron-scale TiO_2 hollow spheres. *Langmuir*, **24**(2):547-550. [doi:10.1021/la702157r]

Liu, Y., Qi, T., Zhang, Y., 2007. Synthesis of hexatitanate and titanium dioxide fibers by ion-exchange approach. *Materials Research Bulletin*, **42**(1):40-45. [doi:10.1016/j.materresbull.2006.05.013]

Lu, H., Zhang, L., Xing, W., Wang, H., Xu, N., 2005. Preparation of TiO_2 hollow fibers using poly (vinylidene fluoride) hollow fiber microfiltration membrane as a template. *Materials Chemistry and Physics*, **94**(2-3):322-327. [doi:10.1016/j.matchemphys.2005.05.008]

Macak, J.M., Schmidt-Stein, F., Schmuki, P., 2007. Efficient oxygen reduction on layers of ordered TiO_2 nanotubes loaded with Au nanoparticles. *Electrochemistry Communications*, **9**(7):1783-1787. [doi:10.1016/j.elecom.2007.04.002]

Madhugiri, S., Sun, B., Smirniotis, P.G., Ferraris, J.P., Balkus, K.J., 2004. Electrospun mesoporous titanium dioxide fibers. *Microporous and Mesoporous Materials*, **69**(1-2):77-83. [doi:10.1016/j.micromeso.2003.12.023]

Matsumoto, A., Tsutsumi, K., Kaneko, K., 1992. Titania coating of a microporous carbon surface by molecular adsorption-deposition. *Langmuir*, **8**(10):2515-2520. [doi:10.1021/la00046a027]

Savage, P.E., 2000. Heterogeneous catalysis in supercritical water. *Catalysis Today*, **62**(2-3):167-173. [doi:10.1016/S0920-5861(00)00418-1]

Viswanathamurthi, P., Bhattarai, N., Kim, C.K., Kim, H.Y., Lee, D.R., 2004. Ruthenium doped TiO_2 fibers by electrospinning. *Inorganic Chemistry Communications*, **7**(5):679-682. [doi:10.1016/j.inoche.2004.03.013]

Yuan, R., Fu, X., Wang, X., Liu, P., Wu, L., Xu, Y., Wang, X., Wang, Z., 2006a. Template synthesis of hollow metal oxide fibers with hierarchical architecture. *Chemistry of Materials*, **18**(19):4700-4705. [doi:10.1021/cm0609911]

Yuan, R., Fu, X., Liu, P., Wang, X., 2006b. Influence of solvents on morphology of TiO_2 fibers prepared by template synthesis. *Scripta Materialia*, **55**(11):1003-1006. [doi:10.1016/j.scriptamat.2006.08.015]

Zeng, H., 2005. Gong Neng Xian Wei (Functional Fibers). Chemical Industry Press, Beijing, p.111.